NMR Studies on Poly(ethylene oxide)-based Polymer Electrolytes with Different Cross-Linking Doped with $LiN(SO_2CF_3)_2$. Restricted Diffusion of the Polymer and Lithium Ion and Time-Dependent Diffusion of the Anion

Kikuko Hayamizu* and Etsuo Akiba

National Institute of Advanced Industrial Science and Technology, AIST Tsukuba Center 5, Tsukuba 305-8565, Japan

Toshinori Bando and Yuichi Aihara

Yuasa Corporation, 4-5-1 Ohgi-cho, Odawara 250-0001, Japan

William S. Price

Department of Chemistry, Tokyo Metropolitan University, 1-1 Minami-Ohsawa, Hachioji, 192-0397, Japan

Received December 4, 2002

ABSTRACT: The reorientational and translational dynamics of the polymer, anion and cation species in polymer electrolyte systems consisting of a cross-linked poly(ethylene oxide−propylene oxide) random copolymer (poly(EO−PO)) doped with $LiN(SO_2CF_3)_2$ at two different cross-linking densities were studied using multinuclear NMR relaxation and pulsed field gradient spin−echo (PGSE) diffusion measurements. Analysis of the data provided exquisite molecular level insight into the individual behaviors of the species. In particular, it was found that in the presence of salt the polymer chains form hyperstructures and that the lithium ions undergo curvilinear diffusion along the chains within these hyperstructures. The anions, on the other hand, diffuse independently of both the polymer and lithium ions, but nevertheless undergo anomalous diffusion due to the effects of diffusing through the microheterogeneous polymer hyperstructure network. The motional behaviors of the three species were reasonably insensitive to the degree of cross-linking but somewhat more sensitive to the salt concentration, since the microcrystallinity of these polymer electrolytes increases with salt concentration.

Introduction

Because of their wide commercial applications including solid-state batteries, there is at present much interest in trying to understand the molecular basis of ionic conductivity in polymer−lithium salt systems.[1] A point of particular interest in such electrolytes is that the ionic transport (and thus conductivity) is decoupled from the macroscopic viscosity. Instead the ionic species have complex dynamics with the lithium transport being closely correlated with its local environment and in particular with the segmental motion of the polymer chains.[2−4] Although it has long been known that the conductivity in such systems is higher in amorphous rather than the crystalline regions, there is now growing realization that even microheterogeneity in macroscopically homogeneous systems significantly affects the conduction processes. Such microheterogeneity must be involved in the transition from the amorphous to the ordered states. Consequently, a deeper understanding of this microheterogeneity is an important step in increasing the conductivity in such systems.

Microheterogeneities with characteristic distances on the order of the diffusive path lengths of a species will affect the diffusive process of the species and consequently species in systems containing microheterogeneities have been observed to undergo anomalous or fractal diffusion over certain length scales.[5−10] The cation and anion diffuse by fundamentally different mechanisms,[2] with the lithium hopping between various coordination sites along the polymer. The polymer segmental motion in turn, modulates this hopping motion. In contrast, the anion hops from an occupied site to a sufficiently large void in the polymer matrix. NMR, through its ability to probe both reorientational and translational motions provides a particularly direct and cogent means of probing the complicated molecular dynamics of ionic conduction in such systems.

We have recently studied a cross-linked poly(ethylene oxide−propylene oxide) random copolymer (poly(EO−PO)), whose precursor macromonomer is a derivative of glycerol bonded to ethylene oxide-*co*-propylene oxide (*m*(EO−PO)) with a molecular weight of about 8000. The terminal OH group was replaced by an acryloyl group ($OCOCH{=}CH_2$) prior to cross-linking. The precursor macromonomers were synthesized in which the acryloyl groups were replaced by methyl groups,[11,12] so that many free chains remained after cross-linking. In the present study, two precursor macromonomers which differed only in their degree of methylation were used: *m*(EO−PO)-M2 (20% methylation) and *m*(EO−PO)-M5 (50% methylation) as shown below in order to prepare cross-linked polymers (i.e., poly(EO−PO)-M2 and the more flexible poly(EO−PO)-M5) of differing flexibilities.

* Corresponding author. E-mail: hayamizu.k@aist.go.jp

10.1021/ma021741i CCC: $25.00
Published on Web 03/19/2003

Higher degrees of methylation were impractical as the resulting cross-linked polymers were unstable.

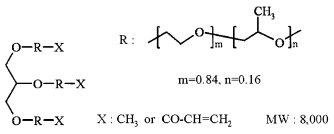

The cross-linked polymers were doped with two different concentrations of $LiN(SO_2CF_3)_2$ and the reorientational and translational motions of all the species were measured using multinuclear NMR relaxation and pulsed gradient spin−echo (PGSE) diffusion measurements, respectively. The results of the ionic conductivity and DSC will be published elsewhere.

Experimental Section

Sample Preparation. The precursor macromonomers, *m*(EO−PO)-M5 and *m*(EO−PO)-M2 were obtained from Daiichi Kogyo Seiyaku, Kyoto and $LiN(CF_3SO_2)_2$ was purchased from Central Glass Co., Ltd, Tokyo. The salt was dissolved in the macromonomers and the solution stirred for 48 h while increasing the temperature to 333 K. After the salt was dissolved completely, the solution was cast on a plate and irradiated with an electron beam (10 Mrad) under nitrogen. Four samples with different salt concentrations were prepared, i.e., Li/O = 0.1 and 0.05 for both poly(EO−PO)-M5 and poly(EO−PO)-M2. Reference samples without salt (i.e., neat) were also prepared. For NMR measurements, the samples were inserted into 5 mm NMR microtubes (BMS-005JA, Shigemi, Tokyo) to a height of 5 mm and flame-sealed. The entire preparation was performed under dry air (moisture < 10 ppm at 213 K). To allow for structural relaxation, the samples were left at room temperature for at least 1 month prior to NMR measurement.

NMR Measurements. The NMR measurements were performed using a JEOL GSH-200 spectrometer with a 4.7 T wide-bore magnet controlled by TecMag Galaxy (subsequently the RF unit was replaced by a TecMag Apollo) system. Most measurements started at 353 K with at least 1 h being allowed prior to measurement to ensure that the samples had achieved thermal equilibrium. The longitudinal and transverse relaxation measurements were performed using the inversion recovery (i.e., 180°−τ−90°−acquisition) and Hahn spin echo (i.e., 90°−τ−180°−τ−acquisition) sequences, respectively. All self-diffusion measurements were performed using a stimulated echo-based PGSE sequence. A JEOL current amplifier was used to generate the magnetic field gradient pulses. The intervals between the first and second RF pulses and the third RF pulse and echo acquisition were fixed to be 5 ms throughout the diffusion measurements. Measurements were performed by adjusting the duration of the gradient pulses (δ). The amplitude of the pulse gradients were 9.2 T m^{-1} for ^{1}H and ^{7}Li diffusion measurements and from 4 to 10 T m^{-1} for the ^{19}F NMR. The reliability of the diffusion measurements was assured by performing crosschecks under more severe conditions to rule out artifacts.[13]

Diffusion Theory

In the short gradient pulse (SGP) approximation, where motion during the gradient pulse is ignored (rigorously, one assumes that $\delta \rightarrow 0$ and $|\mathbf{g}| \rightarrow \infty$ while their product remains finite; experimentally, this requires $\delta \ll \Delta$), the PGSE attenuation is given by[14]

$$E(\mathbf{q},\Delta) = \int\int \mathrm{d}\mathbf{r}_0\, \mathrm{d}\mathbf{r}\, \rho(\mathbf{r}_0) G(\mathbf{r}_0|\mathbf{r};\Delta) \mathrm{e}^{\mathrm{i}2\pi\mathbf{q}\cdot(\mathbf{r}-\mathbf{r}_0)} \quad (1)$$

where $\rho(\mathbf{r}_0)$ is the equilibrium spin density and $G(\mathbf{r}_0|\mathbf{r};\Delta)$ is the Green's function (or diffusion propagator). $\mathbf{q} = (2\pi)^{-1}\gamma\mathbf{g}\delta$ (m^{-1}), γ is the gyromagnetic ratio, and Δ is the separation between the leading edges of the gradient pulses and defines the time scale of the diffusion measurement. In the case of free isotropic diffusion of a single species the signal attenuation is given by

$$E(\mathbf{q},\Delta) = \exp(-4\pi^2 q^2 D\Delta) \quad (2)$$

or, if the effects of the finite duration of gradient pulses are accounted for[15,16]

$$E = \exp(-\gamma^2 g^2 \delta^2 D(\Delta - \delta/3)) \quad (3)$$

As will be seen below, diffusion measurements of some samples provide evidence of motional restriction. The geometrically simplest case is that of diffusion in a reflecting sphere of radius a for which the normalized eigenfunctions of index κ are given by[17]

$$K_\kappa(\mathbf{r}) = \begin{cases} V^{-1/2} & \kappa = 0 \\ \dfrac{1}{\sqrt{N_\kappa}} (\alpha_\kappa r)^{-1/2} J_{n+1/2}(\alpha_\kappa r) P_n(\mu) & \kappa > 0 \end{cases} \quad (4)$$

where V is the volume of the sphere and

$$N = \frac{2\pi}{2n+1} \frac{1}{\alpha_\kappa^3} [(\alpha_\kappa a)^2 - n^2 - n] J_{n+}{}^1/_2(\alpha_\kappa a)^2 \quad (5)$$

where the values of α_κ are determined from the Bessel function equation

$$\frac{n}{\beta_{n,m}} J_{n+1/2}(\beta_{n,m}) = J_{n+3/2}(\beta_{n,m}) \quad (6)$$

The roots, $\beta_{n,m} = \alpha_\kappa a$, are placed in ascending order and indexed by κ. In the SGP limit the PGSE attenuation is given by[18,19]

$$E(\mathbf{q},\Delta) = \frac{9[2\pi qa\cos(2\pi qa) - \sin(2\pi qa)]^2}{(2\pi qa)^6} + 6(2\pi qa)^2 \sum_{\kappa=0}^{\infty} \frac{(2n+1)\beta_\kappa{}^2 j_n'(2\pi qa)^2 \mathrm{e}^{-D(\beta_\kappa{}^2/a^2)\Delta}}{(\beta_\kappa{}^2 - n^2 - n)(\beta_\kappa{}^2 - (2\pi qa)^2)^2} \quad (7)$$

where $j_n(x)$ is a spherical Bessel function. A mathematical derivation for dealing with the case when the SGP limit is not strictly enforced is given in the Appendix. However, for the present experimental parameters it was found that the deviation from the SGP PGSE profile was nearly negligible. Consequently, the (computationally more efficient) SGP solution was used for all simulations of the experimental data.

Even in cases where the form of $G(\mathbf{r}_0|\mathbf{r};\Delta)$ is unknown, expansion of eq 1 reveals that for small q with respect to the characteristic distance of the restricting geometry, R, the echo attenuation is given by

$$E(\mathbf{q} \ll R^{-1}, \Delta) \approx 1 - \frac{(2\pi q)^2 \langle z^2(\Delta)\rangle}{2} \quad (8)$$

where $\langle z^2(\Delta)\rangle$ is the mean squared displacement. In such cases the PGSE data can be analyzed on the basis of an effective diffusivity[7,8,20]

$$D_{\mathrm{eff}}(\Delta) = \frac{\langle z^2(\Delta)\rangle}{2\Delta} \quad (9)$$

Table 1. Activation Energies (kJ mol^{-1}) for the Reorientational and Translational Dynamics of the Polymer Electrolyte Species[a]

electrolyte system	segmental motion	^{7}Li hopping motion	anion reorientation	anion diffusion
poly(EO−PO)-M2	23.0 ± 0.5 (high *T*) 21.0 ± 1.3 (low *T*)			
poly(EO−PO)-M5	21.9 ± 0.5 (high *T*) 21.1 ± 0.9 (low *T*)			
poly(EO−PO)-M2:Li/O=0.05	20.5 ± 0.3	24.2 ± 0.6	12.4 ± 0.3	36.0 ± 2.7
poly(EO−PO)-M5:Li/O=0.05	18.5 ± 0.4	25.4 ± 0.7	13.8 ± 0.4	39.3 ± 1.0
poly(EO−PO)-M2:Li/O=0.1	22.2 ± 0.5	24.3 ± 2.5	9.8 ± 0.3	46.4 ± 1.4
poly(EO−PO)-M5:Li/O=0.1	21.3 ± 1.0	23.3 ± 0.9	10.1 ± 0.3	46.6 ± 1.6

[a] The higher of the two values for the segmental motion of the neat polymers represent a lower temperature range with respect to the discontinuity.

Thus, we have

$$D_{\mathrm{eff}}(\Delta) \propto \Delta^{2/d_w-1} \tag{10}$$

where d_w is the walk dimension. In the case of normal diffusion $2/d_w = 1$, but in the case of anomalous diffusion $2/d_w \leq 1$.

All numerical simulations in the present paper were performed using MathCad (Mathsoft).

Results

Polymer Molecular Dynamics. Relaxation. In each sample, the ^{1}H NMR longitudinal relaxation of the polymer was well described by a single-exponential function of the reorientational correlation time (τ_c) for the segmental motions of the CH_2CH_2O chains. Arrhenius plots of the T_1 values of the main CH_2CH_2O resonance are shown in Figure 1a. The methyl resonances had similar relaxation profiles but with slightly longer values. The Bloembergen, Purcell and Pound (BPP) equation[21] describing homonuclear spin−lattice relaxation by the dipole−dipole interaction is given by

$$\frac{1}{T_1} = A\left(\frac{\tau_c}{1+\omega_0{}^2\tau_c{}^2} + \frac{\tau_c}{1+4\omega_0{}^2\tau_c{}^2}\right) \tag{11}$$

where

$$A = \frac{3}{10}\gamma^4\hbar^2\sum_j \frac{1}{r_j{}^6} \tag{12}$$

and r is the separation between dipoles (e.g., the H−H distance), ω_o is the observed frequency (rad s^{-1}), τ_c is the reorientational correlation time of the dipolar interaction, and the summation index j is over all interacting dipoles. Although, the BPP model is undoubtedly an oversimplification of what is in reality quite a complicated relaxation mechanism. It nevertheless provides a basic framework, which allows reasonable interpretation of the polymer relaxation data.

In the model, due to the term in brackets in eq 11 the spin−lattice relaxation time is a minimum when $\omega_o\tau_c = 2\pi\nu_0\tau_c = 0.616$. In the current study the ^{1}H observed frequency, ν_0, is 199.76 MHz and the numerical calculation of the term in brackets in eq 11 was possible at the T_1 minimum point. From the observed T_1 minimum, the constant term A in eq 12 can be calculated. The evaluation of correlation time, τ_c, was made from the T_1 observed at each temperature. The calculated values of τ_c are plotted in Figure 1b together with the τ_c values for the lithium hopping motions (see below) and the corresponding activation energies are tabulated in Table 1. Previously we described the relaxation mechanisms of the ^{1}H resonance by the proton−proton interactions between the neighboring protons for the poly(EO−PO) electrolytes.[2]

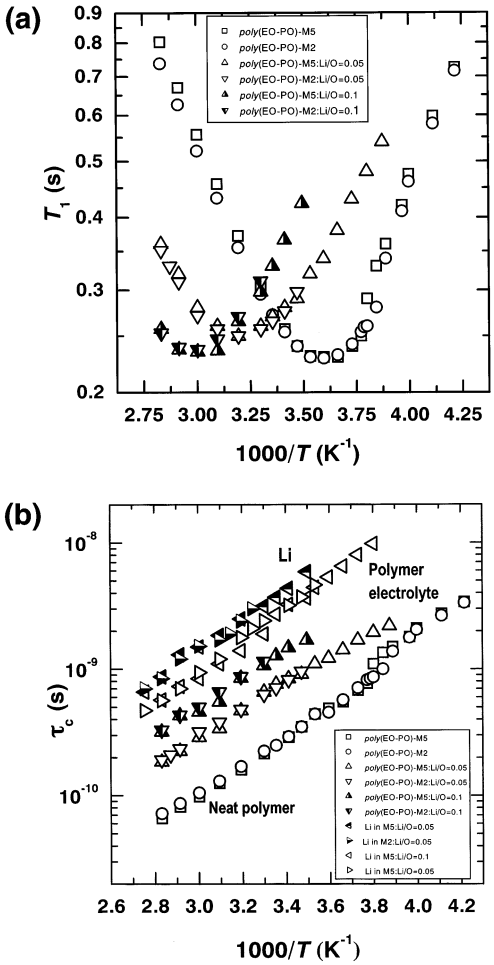

Figure 1. (a) Temperature dependencies of the ^{1}H T_1 in the neat poly(EO−PO)-M2 (circle) and poly(EO−PO)-M5 (square) and doped poly(EO−PO)-M2 (down-triangle) and M5 (up-triangle). (b) The temperature dependence of the correlation times for the polymer segmental motions and the lithium hopping motions.

Although the relaxation profiles are continuous for the doped polymers, discontinuities, indicating some form of abrupt structural transition, were observed for the neat polymer samples around 270 K and also in the plots of the correlation time. Although the segmental motions were reduced as the salt concentration increased (i.e., τ_c became longer), the activation energies were unaffected and range between 18 and 23 kJ mol^{-1}

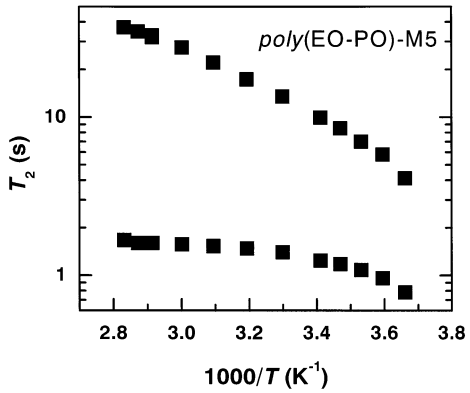

Figure 2. Biexponential analysis of the ^{1}H Hahn spin−echo decays for the undoped poly(EO−PO)-M5 between 358 and 273 K.

for the six samples. These values are similar to those for the segmental motions in cross-linked polyethers,[2,22] viscous liquid macromonomers,[4] and liquid glyme families and poly(ethylene glycol) dimethyl ethers.[23]

In contrast to the ^{1}H longitudinal relaxation, the transverse relaxation appeared to be a biexponential process. The proportion of the longer component increased as the degree of cross-linking decreased and the salt concentration decreased. Although the amplitude and time constants of the two transverse relaxation components of the salt-free polymers (poly(EO−PO) and poly(EO−PO)-M2) exhibited only a small temperature dependence, a much larger difference was observed for poly(EO−PO)-M5 (see Figure 2). Curiously, the echo decay of poly(EO−PO)-M2 was temperature insensitive with the two components having relative amplitudes of 0.8 and 0.2 with T_2 values of 0.8 and 8 ms, respectively. The temperature dependence of the transverse relaxation behavior of the doped-polymers were similar to the neat poly(EO−PO)-M5. The echo signals of the major component having the shorter T_2 had completely decayed by around 20 ms for all the samples in the present study.

Diffusion. The analysis of the PGSE diffusion measurements is complicated by the heterogeneity of the polymer systems with the ensuing uncertainty as to the number of components. Since the PGSE sequence is echo-based, the diffusion coefficients determined will be weighted in favor of the (more slowly relaxing) flexible parts of the polymers. Since the major component of the echo decayed rapidly, the PGSE measurements of each of the two neat polymers were reflected on the smaller component with the longer relaxation time. The PGSE attenuation profiles were single-exponential and the diffusion coefficients obtained by regressing eq 3 onto the data obtained with various Δ values in the temperature range between 353 and 303 K are given in Figure 3a. Interestingly, the coefficients were independent of both temperature and the degree of methylation. The observed Δ dependence of the diffusion coefficients is likely the result of the changing contribution of the various components due to the relaxation weighting inherent in the pulse sequence. Nevertheless, the data could be well described by eq 10 with values of $2/d_w$ ranging between 0.44 and 0.46.

In contradistinction to the neat polymers, the PGSE attenuation profiles of the doped polymers were always nonexponential and thus indicative of restricted diffusion as shown for poly(EO−PO)-M2:Li/O=0.05 in Figure 3b. At shorter Δ there was clear evidence of diffractive minima resulting from restricted diffusion. For the SGP sphere model, the first diffractive minimum occurs when $q \cong 0.71/a$. The radii of restriction calculated were given by 0.97, 1.1, and 1.07 μm for the Δ = 30, 50, and 100 ms data sets, respectively. The profiles only approached exponential at Δ = 200 ms giving an apparent free diffusion coefficient of 8×10^{-13} m^2 s^{-1}, which is similar to the coefficients of the neat samples. With the radius set to be 1 μm, nonlinear least-squares regression was used to determine the optimum values of D. The values were 3.2×10^{-12}, 2.5×10^{-12}, 1.8×10^{-12}, and 1.8×10^{-12} m^2 s^{-1} for Δ = 30, 50, 100, and 200 ms, respectively. The value at Δ = 200 ms is an overestimate of D compared with that obtained using eq 3. There are two points of interest, first the apparent diffusion coefficient decreases with Δ—as observed for the neat polymers. Second, these values give mean-square displacements considerably less than 1 μm. Consequently, theoretical profiles calculated using the sphere model with these values, although nonexponential, do not give diffraction minima. Finally the experimental diffractive minima are rather shallow. Shallow minima are signatures of polydispersity of the characteristic size (i.e., a) of the restricting geometry.[24] However, the inclusion of significant polydispersity gives almost negligible effect on the calculated profiles since the mean-square displacements are considerably less than the apparent radius of the restricting geometries.

Measurements were performed for poly(EO−PO)-M5: Li/O=0.1 at various temperatures at a fixed value of Δ (100 ms) and within experimental error no temperature dependence was observed (see Figure 3c). Setting the radius to be 0.9 μm, the optimum value of D was 9.1×10^{-13} m^2 s^{-1} and the simulation is given in the figure. As noted above, such a small diffusion coefficient is unable to generate diffusive minima using the sphere model. In fact, reasonable diffractive behavior only becomes apparent when the diffusion coefficient is almost an order of magnitude faster and an identical simulation but with $D = 8.0 \times 10^{-12}$ m^2 s^{-1} which exhibits diffractive minima is also given in the figure (NB giving a mean-square displacement of ~1.3 μm). However, apart from allowing generation of diffractive minima, the higher diffusion coefficient results in a much poorer fit to the data, as the echo attenuation is greatly overestimated. PGSE profiles of the four electrolytes derived from poly(EO−PO)-M5 and poly(EO−PO)-M2 at 333 K with Δ = 100 ms are shown in Figure 3d. Apart from the poly(EO−PO)-M2:Li/O=0.1 sample, the four plots are quite similar with diffractive minima which give the radius of restriction as being 1.1 μm. The poly(EO−PO)-M2:Li/O=0.1 sample, however, has a diffractive minimum which gives the radius as 1.3 μm. Using these values of a, the calculated diffusion coefficients were (M2:Li/O = 0.05) 1.73×10^{-12} m^2 s^{-1}, (M2:Li/O = 0.1) 1.88×10^{-12} m^2 s^{-1}, (M5:Li/O = 0.05) 1.46×10^{-12} m^2 s^{-1}, and (M5:Li/O = 0.1) 1.22×10^{-12} m^2 s^{-1}. Thus, the polymer diffusion is reasonably insensitive to both the salt concentration and degree of cross-linking.

Three Lithium Ion Molecular Dynamics. The longitudinal relaxation of the single ^{7}Li resonance was single exponential and the temperature dependence of the T_1 values are plotted in Figure 4. The T_1 minima (~ 0.16 s) were observed at around 318 K for Li/O = 0.05 samples and around 343 K for the Li/O = 0.1 samples. The T_1 values of the ^{7}Li ions ($I = {}^3/_2$) under-

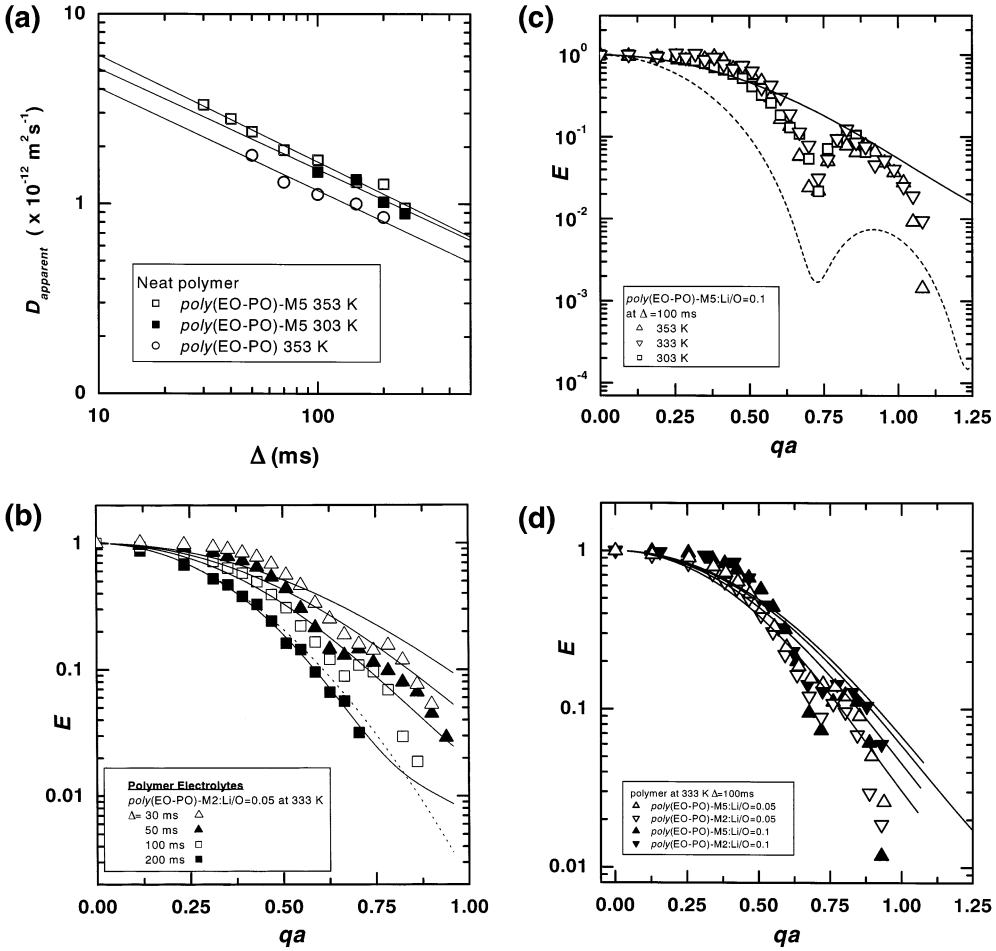

Figure 3. (a) Apparent diffusion coefficients of the neat polymers vs Δ for poly(EO−PO)-M5 at 353 K (open square) and 303 K (solid square) and poly(EO−PO) at 353 K (open circle). The solid lines are the result of regressing eq 10 onto the data. (b) ^{1}H PGSE attenuation profiles for poly(EO−PO)-M2:Li/O=0.05 at 333 K for various Δ values, 30 (open triangle), 50 (solid triangle), 100 (open square), and 200 ms (solid square). The solid and dashed lines denote simulations of the data using the free diffusion and SGP sphere models (eq 7 with a = 1.0 μm), respectively. (c) ^{1}H PGSE attenuation profiles of poly(EO−PO)-M2:Li/O=0.1 obtained with Δ = 100 ms at 303 (square), 333 (down-triangle), and 353 K (up-triangle). The solid and dashed lines denote simulations using the SGP sphere model with a = 0.9 μm and D = 9.1 × 10^{-13} m^2 s^{-1} and 8.0 × 10^{-12} m^2 s^{-1}, respectively. (d) ^{1}H PGSE attenuation profiles of the electrolytes of poly(EO−PO)-M2 and poly(EO−PO)-M5 at the two salt concentrations obtained with Δ = 100 ms at 333 K.

going isotropic reorientational diffusion can be related to τ_c by[25]

$$\frac{1}{T_1} = \frac{\omega_Q^2}{50}\left(\frac{\tau_c}{\omega_0^2\tau_c^2} + \frac{\tau_c}{1 + 4\omega_0^2\tau_c^2}\right) \qquad (13)$$

where $\omega_q = 2\pi\nu_q$ is the quadrupolar coupling constant. Similar to the analysis for the ^{1}H dipole−dipole relaxation above, the relaxation minimum should occur when $\omega_0\tau_c = 2\pi\nu_0\tau_c = 0.616$ (for ^{7}Li ν_0 = 77.63 MHz). The correlation times of the lithium hopping motions were calculated from the lithium T_1 in a similar way as the segmental motions of the polymer chains described above and plotted vs temperature in Figure 1b. The corresponding activation energies for the reorientational motion determined by Arrhenius analysis are presented in Table 1. The activation energies of the lithium hopping motion are always a little larger than the those of the segmental motions in electrolytes composed of cross-linked polymers, the liquid macromonomers, glymes, and the poly(ethylene glycol) dimethyl ethers.[2,4,22,23]

The ^{7}Li echo decays of the other samples were biexponential (typically $T_{2short} \approx 3.2$ ms and $T_{2long} \gtrsim 40$ ms, with T_{2long} being slightly temperature dependent) and insensitive to the degree of methylation, salt concentration and temperature. Nevertheless, the difference in T_2 values between the components was much

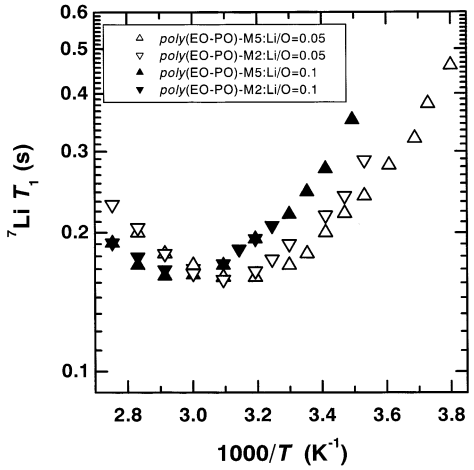

Figure 4. Arrhenius plots of the ^{7}Li T_1 and for poly(EO−PO)-M2 (down-triangle) and -M5 (up-triangle) at the salt concentration of Li/O = 0.05 (open) and 0.1 (solid).

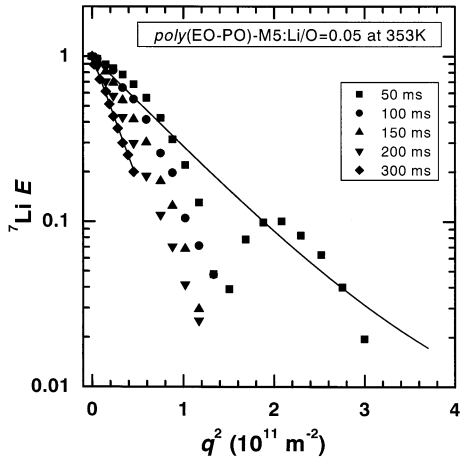

Figure 5. The ^{7}Li PGSE attenuation of poly(EO−PO)-M5: Li/O=0.05 sample at 353 K with various Δ values. The straight line represents the fit to the Δ = 300 ms data using the free diffusion model and the curved line represents the line of best fit to the Δ = 50 ms data using the SGP sphere model.

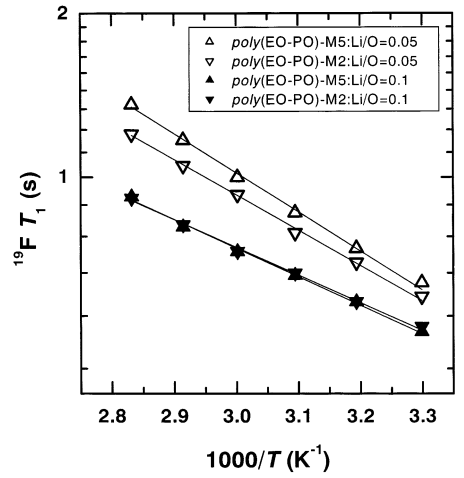

Figure 6. ^{19}F T_1 of the anions for poly(EO−PO)-M2 (down-triangle) and -M5 (up-triangle) with salt concentrations of Li/O = 0.05 (open) and 0.1 (solid). The solid lines are the results of Arrhenius activation analysis.

smaller than those for the ^{1}H decays of the polymers shown in Figure 2a.

The ^{7}Li PGSE attenuation profiles of poly(EO−PO)-M5:Li/O=0.05 obtained at 353 K using various values of Δ are plotted in Figure 5. At short Δ there was clear evidence of a diffractive minimum. Analysis of the Δ = 50 ms data using the SGP sphere model gave the radius of restriction to be 1.9 μm with a corresponding diffusion coefficient of 9.5×10^{-12} m^2 s^{-1}. The profiles only approached single exponential at very long Δ values and at Δ = 300 ms an apparent diffusion coefficient of 3.0×10^{-12} m^2 s^{-1} was obtained. The positions of the diffractive minima were also insensitive to temperature.

Two Anion Molecular Dynamics. The temperature dependence of the anion (i.e., $N(SO_2CF_3)_2$) ^{19}F T_1 values (NB the decays were single exponential) are shown in Figure 6. The T_1 of the Li/O = 0.1 samples were shorter than those of the Li/O = 0.05 samples and, within experimental error, insensitive to the degree of cross-linking. This insensitivity is not surprising since the relaxation of the CF_3 group predominantly results from

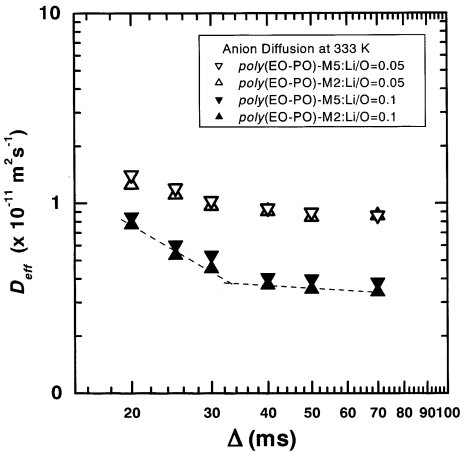

Figure 7. Δ dependence of the apparent self-diffusion coefficient of the anion at 333 K. The symbols are the same as in Figure 6. The dotted lines are the results of regressing eq 10 onto the first and last three data points of the poly(EO−PO)-M2:Li/O=0.1 data set, giving $2/d_w = -0.4$ and 0.9, respectively.

rapid internal rotation around the 3-fold symmetrical axis. The T_1 values for the Li/O = 0.1 samples are nearly identical whereas the T_1 values of the Li/O = 0.05 samples tend to converge with increasing temperature. While the activation energies for the reorientational motion (see Table 1) were nearly identical for the Li/O = 0.1 samples, they were much higher for the Li/O = 0.05 samples with activation energies of 12.4 and 13.8 kJ mol^{-1} for the M2 and M5 samples, respectively.

As previously observed in related systems, the ^{19}F PGSE attenuation profiles are always single exponential and thus consistent with a single isotropically diffusing species, yet the measured diffusion coefficients are Δ-dependent and reach stable "long-time" values by about Δ = 70 ms (Figure 7). The anions diffuse faster in the Li/O = 0.05 samples than in the Li/O = 0.1 samples with the diffusion being a little faster in the (less cross-linked) M5 sample. The Δ dependence of the diffusion changes with Δ and is particularly pronounced in the Li/O = 0.1 samples. At short Δ, $2/d_w$ is $\ll 1$ and approaches 1 with increasing Δ (see the analysis of poly-(EO−PO)-M2:Li/O=0.1 in Figure 7). The activation energies determined from the temperature dependence of the long-time anion diffusion coefficients (Δ = 70 ms) are summarized in Table 1.

Discussion

The molecular level details of the complicated molecular dynamics responsible for the nonideal conductivity behavior of these polymer electrolytes are far from clarified. From the NMR spin−lattice relaxation time and the diffusion measurements of the anion (^{19}F NMR), it is clear that the anion dynamics (both reorientational and translational) are quite independent of both the lithium ion and the polymer (NB the differences in activation energies in Table 1). The dynamics of the lithium ions, however enter into a form of "symbiotic" relationship with the polymer, with the lithium dynamics being modulated by transient binding to chelation sites on the polymer side chains which are themselves undergoing segmental motion. In turn, the lithium ions form transient salt bridges between the polymer segments, which modulate the dynamics of the polymer chain. The close relationship between the lithium hop-

ping and polymer segmental motions is clearly shown in Figure 1b. The order of the τ_c values is (slowest to fastest) lithium < doped polymer < polymer. The motions are slowed as the salt concentration increased.

The neat polymer diffusion measurements report on motions that occur on a completely different more "macroscopic" time scale than the relaxation measurements. Although the PGSE attenuation profiles of the neat polymers appear exponential and thus consistent with the isotropic diffusion of a single component, the Δ dependence indicates that the diffusion is non-Fickian. The Δ dependence of the diffusion behavior is close to that expected for regime III of the Doi−Edwards model of polymer reptation (i.e., $2/d_w \sim -1/2$).[7,26]

Anomalous diffusion due to restriction can be ruled out by virtue of the exponential PGSE profiles observed. Since the translational diffusion of the cross-linked positions is more retarded and consequently the cross-linked positions have the role of anchor, the diffusion of the flexible chains must be somewhat restricted to within a domain.

When doped with lithium salt the polymer PGSE attenuation profiles are clearly nonexponential, indicating some form of motional restriction of the polymer diffusion, and indeed show diffractive minima. Assuming (the simplest case) of a spherical restriction, analysis of the first diffractive minimum implies a restriction with a radius of around 1 μm. We note that similar sized restrictions have been observed in the case of aqueous solutions of the triblock polymer poly(EO)−poly(PO)−poly(EO).[5] In that study it was suggested that the restriction was correlated with the grain boundaries of polycrystalline structures formed from micelles of the triblock polymer. Although the present system is chemically distinct (i.e., no micelle formation), the diffusion data nevertheless indicates the formation of structures much greater than that of the component polymer molecules. Compared to the neat polymer, the restricted diffusion observed in the doped polymer clearly indicates the lithium induces the formation of additional cross-links in the flexible portion of the side chains.

Similar to the doped-polymer diffusion profiles, the diffusion of the lithium also displays evidence of restriction, but the apparent radius of restriction is seemingly twice as large ($\sim$2 μm). For both species the profiles became more exponential at longer Δ. However, using the long Δ diffusion coefficients of the species, the mean square displacements (e.g., for of Li in poly(EO−PO)-M5-:Li/O=0.05, $D = 8 \times 10^{-12}$ m^2 s^{-1} which gives a mean square displacement of 1.3 μm over $\Delta = 100$ ms) are less than the radius of restriction. One reason for this inconsistency might be that the lithium ions undergo curvilinear diffusion along the polymer chains (e.g., see ref 27), and if the chance of hopping between hyperstructures is low, they will appear to be geometrically restricted and thus their PGSE profiles exhibit diffractive minima. Diffractive minima only become apparent when the long time limit is approached (i.e., a Δ value sufficiently long for the diffusing species to probe all of the geometry restricting it).

In this limit only the first term in eq 7 (i.e., the zero-order eigenvalue) is relevant and consequently the attenuation profile becomes independent of D. Hence, the temperature independence of the diffractive minima indicate that the size of the hyperstructures is temperature independent. Thus, the diffusion measurements provide evidence of the formation of large scale "hyperstructures" which infer both anomalous diffusion behaviors on the lithium ion and polymer but also restricted diffusion effects. However, if the "walls" of the restriction are not truly reflecting (i.e., porous), then, at even longer Δ, the PGSE experiment will probe motion on length scales greater than the restrictive geometries and apparent free diffusion phenomena will be observed (e.g., see the Li diffusion data in Figure 5) as the effects of the short time restrictions will be "smoothed out".

The diffusion of the anions is quite different from either the polymer or the lithium ion. The Δ dependence of the apparent anion diffusion coefficient changes from anomalous at shorter Δ to Fickian at longer Δ with the point of transition being around $\Delta = 30$ ms for the Li/O = 0.1 samples. This corresponds to a mean squared displacement of the anions of about 1 μm—which is on the length scale of the hyperstructures. The Δ dependence of the diffusion is much less evident in the Li/O = 0.05 samples. Thus, we presume that the addition of the salt increases the microcrystallinity of the sample and thus the greater Δ dependence of the diffusion in the Li/O = 0.1 samples is a direct reflection of the transient microheterogeneity present.

Conclusions

The cross-linked (poly(EO−PO))−$LiN(SO_2CF_3)_2$ electrolytes have both liquid and solid like properties, which is to be expected as small perturbations in composition and conditions can change the physical form from amorphous to ordered states. The experimental data lead to a picture of the lithium salt almost completely dissociating in the polymer matrix. The lithium ions induce the polymer molecules to form fluctuating hyperstructures. Induced by the polymer segmental motions, the rapidly hopping lithium ions undergo curvilinear diffusion along the polymer chains within these hyperstructures. However, the anions, which are rather independent of both the polymer and lithium ions, exhibit anomalous diffusion over certain length scales due to the effects of diffusing through the microheterogeneous polymer network. We surmise that the time needed for structural relaxation of these polymer electrolytes before consistent NMR results can be obtained is related to the formation and equilibrium of the hyperstructures.

Appendix

When the short gradient pulse limit does not apply, the attenuation can be calculated using a matrix formulation[28] in which the PGSE sequence is discretized into $2N+1$ intervals of length τ (not the τ in the relaxation sequences) such that the total length of the sequence is $(2N + 1)\tau$. Using this discretization we have

$$\Delta = \left(N + \frac{1}{2}\right)\tau \tag{14}$$

and

$$\delta = \left(M + \frac{1}{2}\right)\tau \tag{15}$$

hence, the total effective q is

$$q_{net} = (M + 1)q_\tau = (M + 1)(2\pi)^{-1}\gamma g\tau \tag{16}$$

$q_{net} = (M + 1)q_\tau = (M + 1)(2\pi)^{-1}\gamma g\tau$, and the matrix equation for the attenuation is

$$E = S(q)[RA(q)]^M R^{N-M}[RA^\dagger(q)]^M RS^\dagger(q) \quad (17)$$

The matrices are given by

$$R_{\kappa\kappa} = \exp(-D\alpha_\kappa{}^2\tau) \quad (18)$$

$$S_\kappa(\mathbf{q}) = \begin{cases} V^{-1}\left[\dfrac{\sin(2\pi qa) - 2\pi qr\cos(2\pi qa)}{2\pi^2 q^3}\right] & \kappa = 0 \\ V^{-1/2}\dfrac{2\pi i^\kappa}{\sqrt{N_\kappa}}(q\alpha_\kappa)^{-1/2}\dfrac{J_{\kappa+1/2}(\alpha_\kappa a)}{\alpha_\kappa{}^2 - (2\pi q)^2}[\kappa J_{\kappa+1/2}(2\pi qa) - & \\ \qquad 2\pi qa J_{\kappa+3/2}(2\pi qa)] & \kappa > 0 \end{cases} \quad (19)$$

$$A_{\kappa,\lambda}(\mathbf{q}) = \begin{cases} S_\lambda(\mathbf{q}) & \kappa = 0, \lambda \neq 0 \\ S_\kappa(\mathbf{q}) & \lambda = 0, \kappa \neq 0 \\ \dfrac{2\pi}{\sqrt{N_\kappa N_\lambda \alpha_\kappa \alpha_\lambda q}}\displaystyle\int_0^a r^{1/2} J_{\kappa+1/2}(\alpha_\lambda r) J_{\lambda+1/2}(\alpha_\lambda r) \times & \\ \qquad \displaystyle\sum_{k=0}^{\lambda} \Xi_k(\kappa,\lambda)\, J_{\kappa+\lambda-2k+1/2}(2\pi qr)\, dr & \kappa, \lambda \neq 0 \end{cases} \quad (20)$$

where λ is used a second index for labeling the eigenvalues (i.e., the same meaning as κ).

$$\Xi_k(\kappa,\lambda) = \frac{a_{\lambda-k}a_k a_{\kappa-k}}{a_{\kappa+\lambda-k}}\left(\frac{2\kappa + 2\lambda - 4k + 1}{2\kappa + 2\lambda - 2k + 1}\right) i^{\kappa+\lambda-2k} \quad (21)$$

where

$$a_l = \frac{(2l-1)!!}{l!}$$

It is possible to evaluate the integral in eq 20 in terms of a triple summation of hypergeometric and Γ functions; however, it is more efficient to numerically evaluate the equation as is.

References and Notes

(1) Tarascon, J. M.; Armand, M. *Nature (London)* **2001**, *414*, 359−367.
(2) Hayamizu, K.; Aihara, Y.; Price, W. S. *J. Chem. Phys.* **2000**, *113*, 4785−4793.
(3) Golodnitsky, D.; Livshits, E.; Ulus, A.; Barkay, Z.; Lapides, I.; Peled, E.; Chung, S. H.; Greenbaum, S. *J. Phys. Chem.* **2001**, *A105*, 10098−10106.
(4) Hayamizu, K.; Sugimoto, K.; Akiba, E.; Aihara, Y.; Bando, T.; Price, W. S. *J. Phys. Chem.* **2002**, *B 106*, 547−554.
(5) Scheller, H.; Fleischer, G.; Kärger, J. *Colloid Polym. Sci.* **1997**, *275*, 730−735.
(6) Walderhaug, H.; Nyström, Bo. *J. Phys. Chem.* **1997**, *B 101*, 1524−1528.
(7) Kärger, J.; Fleischer, G.; Roland, U. *Diffusion in Condensed Matter*; Vieweg: Braunschweig, Germany, 1998; Chapter 6, pp 144−168.
(8) Ben-Avraham, D.; Havlin, S. *Diffusion and Reactions in Fractals and Disordered Systems*; Cambridge: Cambridge, England, 2000.
(9) Azurmendi, H. F.; Ramia, M. E. *J. Chem. Phys.* **2001**, *114*, 9657−9662.
(10) Malcai, O.; Lidar, D. A.; Biham, O.; Avnir, D. *Phys. Rev.* **2002**, *E 56*, 2817−2828.
(11) Watanabe, M.; Nishimoto, A. *Solid State Ionics* **1995**, *79*, 306−312.
(12) Kono, M.; Hayashi, E.; Watanabe, M. *J. Electrochem. Soc.* **1998**, *145*, 1521−1526.
(13) Price, W. S.; Hayamizu, K.; Ide, H.; Arata, Y. *J. Magn. Reson.* **1999**, *139*, 205−212.
(14) Stejskal, E. O. *J. Chem. Phys.* **1965**, *43*, 3597−3603.
(15) Stejskal, E. O.; Tanner, J. E. *J. Chem. Phys.* **1965**, *42*, 288−292.
(16) Price, W. S. *Concepts Magn. Reson.* **1997**, *9*, 299−336.
(17) Carslaw, H. S.; Jaeger, J. C. *Conduction of Heat in Solids*, 2nd ed.; Oxford University Press: Oxford, England, 1959.
(18) Balinov, B.; Jönsson, B.; Linse, P.; Söderman, O. *J. Magn. Reson.* **1993**, *A 104*, 17−25.
(19) Balinov, B.; Jönsson, B.; Linse, P.; Söderman, O. *J. Magn. Reson.* **1994**, *A 108*, 130.
(20) Vojta, G.; Renner, U. *Diffusion in Condensed Matter*; Vieweg: Braunschweig, Germany, 1998; Chapter 13, pp 306−318.
(21) Bloembergen, N.; Purcell, E. M.; Pound, R. V. *Phys. Rev.* **1948**, *73*, 679−712.
(22) Hayamizu, K.; Aihara, Y.; Price, W. S. *Electrochim. Acta* **2001**, *46*, 1475−1485.
(23) Hayamizu, K.; Akiba, E.; Bando, T.; Aihara, Y. *J. Chem. Phys.* **2002**, *117*, 5929−5939.
(24) Price, W. S.; Stilbs, P.; Söderman, O. *J. Magn. Reson.* **2003**, *160*, 139−143.
(25) Werbelow, L. G. *Encyclopedia of Nuclear Magnetic Resonance*; Wiley: New York, 1996; pp 4092−4101.
(26) Appel, M.; Fleischer, G.; Kärger, J.; Fujara, F.; Chang, I. *Macromolecules* **1994**, *27*, 4274−4277.
(27) Ambrosone, L.; Angelico, R.; Ceglie, A.; Olsson, U.; Palazzo, G. *Langmuir* **2001**, *17*, 6822−6830.
(28) Callaghan, P. T. *J. Magn. Reson.* **1997**, *129*, 74−84.

MA021741I